PHYSICAL REVIEW B VOLUME 18, NUMBER 1 1 JULY 1978

Diffusion of hydrogen in niobium in the presence of trapping impurities studied by neutron spectroscopy

D. Richter
Institut für Festkörperforschung, KFA Jülich, D-517 Jülich, West Germany

T. Springer
Institut Laue-Langevin, F-38042 Grenoble-Cédex, Boîte Postale 156 France
and Institut für Festkörperforschung, KFA Jülich, D-517 Jülich, West Germany
(Received 10 June 1977)

The diffusion of hydrogen in niobium with interstitial impurities was investigated by high-resolution neutron spectroscopy for the system NbN_xH_y with $x=0.4$ and 0.7 at.% and $y=0.4$ and 0.3 at.%, respectively. The neutron spectrum at larger scattering vector $\vec{Q}$ consists of two parts: a narrow line centered at energy transfer $\hbar\omega=0$ (width 0.1–3 μeV) which is caused by hydrogen trapped on nitrogen atoms, and a broad component in the spectrum from hydrogen atoms which diffuse in the more or less undisturbed regions of the lattice. At small $\vec{Q}$, the spectral width is directly related to the self-diffusion constant. The experimental spectra, measured as a function of temperature and scattering vector, were interpreted by two theoretical models: (i) a two-state random-walk model (RWM) where the hydrogen alternates between a trapped state and a state of undisturbed diffusion. The RWM is characterized by the mean escape rate from the trap $1/\tau_0$, and the capture rate on the traps $1/\tau_1$; and (ii) an elastic-continuum model: the nitrogen-hydrogen interaction is treated in terms of the elastic strain field produced by the interstitial nitrogen and hydrogen atoms, and in terms of a short-range hard-core repulsion. This model uses the elastic parameters of the niobium and the interstitial nitrogen and hydrogen atoms. The hard-core radius r_0 is the only disposable parameter of the model. The RWM should hold as long as $2\pi/\vec{Q}$ is larger than the linear dimensions of the trapping region. Model (i) yields a very good and consistent description of the measured spectra as a function of the concentration x, the temperature and the scattering vector. The resulting parameters τ_0 and τ_1 have the predicted behavior. In particular, τ_0 is independent of x, and τ_1^{-1} is proportional to $xD(T)$ where D is the self-diffusion constant in pure niobium. The trapping times are about two orders of magnitude larger than the mean rest time in pure niobium. Using a hard-core radius of $r_0 \simeq 2.3$ Å, model (ii) describes very well the experimental spectra at small and large $\vec{Q}$ values.
PACS numbers 66.30.Jt 1977 BF1034

I. INTRODUCTION

Numerous investigations have demonstrated that the physical properties of hydrogen dissolved in transition metals are strongly changed by the presence of small amounts of interstitial impurities, in particular the hydrogen solubility and its self-diffusion constant. These observations have an intrinsic physical interest in view of the thermodynamics and kinetics of the hydrogen-metal systems.

Observations in this field have shown that interstitial impurities as N, O, or C tend to increase the hydrogen solubility[1–3] and that they reduce the self-diffusion coefficient.[4] Furthermore, the residual resistivity per dissolved hydrogen atom is diminished by the presence of dissolved nitrogen.[5] Finally, oxygen or nitrogen impurities in the niobium-hydrogen system are responsible for additional relaxation maxima of the internal friction.[6–8] All these observations can be naturally explained by the assumption that impurities act as trapping centers for the dissolved hydrogen. This means that they cause a lowering of the ground-state energy of the hydrogen atom in the vicinity of the interstitial, and, correspondingly, an increase of the barrier height for the diffusive motion. Obviously, this enhances the solubility, and, as well, reduces the diffusive jump rate. Furthermore, trapping implies the formation of hydrogen-impurity pairs. They are assumed to scatter the conduction electrons with a smaller probability than the isolated interstitials. Such N-H pairs may be also responsible for the relaxation processes mentioned before.

In the present work we studied the influence of the trapping process caused by nitrogen impurities on the

diffusive motion of hydrogen in niobium by incoherent scattering of slow neutrons. The aim of the investigation was an atomistic understanding of the trapping and its influence on diffusion, and the development of simple theoretical models for a quantitative description of these effects. The system Nb-N-H was chosen because niobium has a particularly small incoherent scattering cross section together with small absorption so that hydrogen scattering is still observable at relatively small hydrogen concentrations. Furthermore, large experience exists in view of the preparation of the samples. The jump rates under consideration are relatively small (10^8–10^{10} sec^{-1}). The corresponding width of the quasielastic neutron spectrum is of the order of a few μeV. Consequently, these experiments could only be carried out by means of a high-resolution backscattering spectrometer.

The experiments were performed at relatively small nitrogen concentrations. Therefore, trapping regions and undisturbed regions in the host material are separated. Under such circumstances, relatively simple arguments can be given to explain what kind of information can be obtained from the scattering experiment: for small momentum transfer of the neutron $\hbar Q$ the scattering process averages over a *large* volume in space (of the order of $(2\pi)^3/Q^3$). Therefore, long sections of the diffusive path of the scattering hydrogen are "observed" by the neutron wave packet propagating through the sample. The path includes periods of nearly undisturbed diffusion, as well as periods where the hydrogen is trapped. It is easy to understand that the width of the quasielastic spectrum at small Q is essentially determined by the effective diffusion coefficient in the nitrogen-doped sample. At large Q however, the average occurs over a small space volume and the quasielastic spectrum depends essentially on a single step of the diffusive motion. In this case, information is obtained about the mean trapping time, and about the fraction of the trapped hydrogen atoms.

In Sec. II of this paper these considerations are formulated quantitatively. For this purpose, the autocorrelation function $G_s(\vec{r},t)$ of the diffusing hydrogen will be calculated. To obtain the scattering spectrum, two simple models will be developed. (i) The *random-walk model* (RWM), where the trap is treated as an isolated "black box" which is surrounded by the undisturbed host lattice, and which is characterized by a *single* trapping time. This model yields simple analytic expressions for the quasielastic spectrum and for the effective diffusion constant. (ii) *The elastic interaction model* which yields a more-detailed description of the problem. It considers the variety of changed ground-state energies and jump rates for the hydrogen atom in the vicinity of the nitrogen impurity. The long-range interaction is treated by anisotropic elastic theory, whereas the short-range part is formulated by a hard-core repulsion.

Section III describes the neutron scattering experiments and the problems related to the preparation and characterization of the Nb-N-H samples. Finally, Sec. IV presents the interpretation of the measured neutron spectra in terms of the two models. As will be seen, the interpretation of the experiments by the random-walk model incorporates the mean trapping time, the capture rate of the trap, and the effective self-diffusion coefficient in the nitrogen-doped sample in a consistent manner. Using only one parameter, namely, the hard-core radius r_0, the elastic-interaction model describes very well the experimental results for the effective diffusion coefficient, as well as, for the linewidth at larger Q values. Furthermore, the model yields more detailed information on the structure of the trap. We want to point out that these experiments could be used to understand the general dynamics of various trapping mechanisms which strongly influence the behavior of materials during radiation damage.[9] Our experiments were the first where the behavior of interstitial atoms in the presence of traps was observed in space and time on a microscopic scale.[10]

II. THEORY

The spectral distribution of slow neutrons scattered on a hydrogen-loaded niobium sample is proportional to the incoherent scattering law $S_{\rm inc}(\vec{Q},\omega)$ which can be presented by a Fourier transform of the van Hove self-correlation function for the motion of the scattering particle $G_s(\vec{r},t)$, namely,[11]

$$S_{\rm inc}(\vec{Q},\omega)=\frac{1}{(2\pi)^3}\int d^3r dt\,\exp[i(\vec{Q}\cdot\vec{r}-\omega t)]G_s(\vec{r},t)\ , \tag{1}$$

where

$$\hbar\omega=E_0-E_1 \quad\text{and}\quad \hbar\vec{Q}=\hbar(\vec{k}_0-\vec{k}_1) \tag{2}$$

are the energy and momentum transfer during scattering, respectively. In our experiments the contribution of coherent scattering from the protons, as well as the scattering from the host lattice can be practically neglected. In calculating the function $G_s(\vec{r},t)$ the oscillatory motion of the diffusing hydrogen atom during the rest time on the interstitial site will be neglected. The assumption is justified since in our experiments only the region of small energy transfers will be studied where acoustic and optic excitation do not appear. Furthermore, it will be assumed that the flight time of the hydrogen between the interstitial sites is small compared to the mean rest time. Under these conditions, the time evolution of the self-correlation function for the diffusive motion of the hydrogen can be described by a system of rate equations, namely,

$$\frac{\partial}{\partial t} G_{\vec{i}}^{\vec{m}}(t) = \sum_{\vec{n}} (\Gamma^{\vec{m}\,\vec{n}} G_{\vec{i}}^{\vec{n}} - \Gamma^{\vec{n}\,\vec{m}} G_{\vec{i}}^{\vec{m}}) \equiv \sum_{\vec{n}} \Lambda_{\vec{m}\,\vec{n}} G_{\vec{i}}^{\vec{n}}(t) \quad , \tag{3}$$

$\vec{m}$ denote the translation vectors of the interstitial lattice. $G_{\vec{i}}^{\vec{m}}(t)$ is the probability to find the scattering proton at a site $\vec{m}$ and a time t if it was, at a time $t=0$, at a site $\vec{i}$. $\Gamma^{\vec{n},\vec{m}}$ is the probability per unit time that a jump takes place from a site $\vec{m}$ to site $\vec{n}$;

$$\tau_{\vec{m}} = \left(\sum_{\vec{n}} \Gamma^{\vec{n}\,\vec{m}} \right)^{-1} \tag{4}$$

is the mean rest time of the hydrogen on an interstitial site $\vec{m}$. $G_{\vec{i}}^{\vec{n}}$ fulfills the initial condition

$$G_{\vec{i}}^{\vec{m}}(0) = \delta_{\vec{m}\,\vec{i}} \rho_{\vec{i}} \quad , \tag{5}$$

where $\rho_{\vec{i}}$ is the thermal occupancy of site $\vec{i}$, namely,

$$\rho_{\vec{i}} = e^{\beta E_{\vec{i}}} / \sum_{\vec{n}} e^{\beta E_{\vec{n}}} \quad , \quad \beta = \frac{1}{k_B T} \quad . \tag{6}$$

The sum has to be carried out over all accessible sites of the host lattice. $E_{\vec{n}}$ is the ground-state energy of the hydrogen which depends on the site $\vec{n}$ in the vicinity of an impurity atom. Formally, the rate equation (3) can be solved and the corresponding scattering law can be calculated.[12] In general, it consists of a superposition of Lorentzians whose widths are the eigenvalues λ_s of the rate equation. Their weights g_s are related to the eigenvectors of the rate equation and to the occupation numbers $\rho_{\vec{i}}$, and the scattering law has the general form

$$S_{\text{inc}}(\vec{Q}, \omega) = \sum_s g_s(\vec{Q}) \frac{\lambda_s/\pi}{\lambda_s^2 + \omega^2} \quad . \tag{7}$$

For an undisturbed Bravais lattice, all sites $\vec{n}$ are equivalent and Eq. (3) yields immediately,[13]

$$S_{\text{inc}}(\vec{Q}, \omega) = \frac{\Lambda(\vec{Q})/\pi}{\Lambda(\vec{Q})^2 + \omega^2} \quad , \tag{8}$$

where $\Lambda(\vec{Q})$ is the Fourier transform of the "jump matrix" $\Lambda_{\vec{m}\,\vec{n}}$. For small Q (Q^{-1} much greater than the jump distance) the half-width is given by

$$\Lambda(\vec{Q}) = DQ^2 \quad . \tag{9}$$

This result does not depend on the lattice type. If Q approaches the zone boundary, the quasielastic width is given by α/τ where the constant α depends on the lattice geometry. In the following, the self-correlation function $G_s(\vec{r},t)$ is calculated approximately for a host lattice with dilute impurities. In its surrounding, the dissolved impurity atom modifies the ground-state energy, as well as the saddle point for the diffusive step of the hydrogen. Figure 1 shows schematically the potential configuration for a H atom in the vicinity of the impurity atom. At short distances the electronic repulsion dominates, whereas at larger distances the elastic interaction comes into play. The whole disturbed region around the impurity (in general characterized by a variety of modified jump rates $\Gamma^{\vec{m}\,\vec{n}}$ and ground-state energies $E_{\vec{n}}$) will be called a "trap."

In the *random-walk model* mentioned in Sec. I, the impurity and its immediate surrounding is treated as a

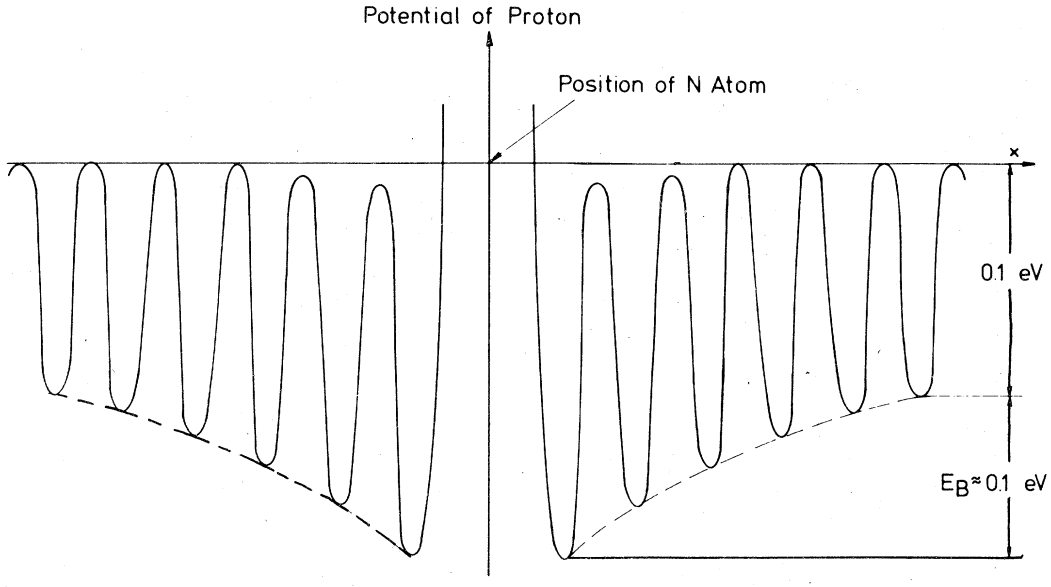

FIG. 1. Schematic sketch of the potential for a proton in the vicinity of a nitrogen impurity. E_B, the binding energy, is the lowest value of the ground-state energy of the proton in the trap (for simplicity, the zero-point energy is neglected in the drawing).

black box which is characterized by a mean trapping time τ_0 of the hydrogen. This implies a description of the complicated time behavior of the hydrogen in the "trap" by a simple exponential, namely,

$$p(t) = \exp(-t/\tau_0) \ , \tag{10}$$

which is the probability of finding the hydrogen in this trap at a time t if it was already there at an earlier time $t=0$. Furthermore, we assume that after escaping the trap, the hydrogen diffuses as in the undisturbed lattice. Correspondingly, for the probability of finding the hydrogen in the diffusive state after a time t has elapsed, one gets

$$q(t) = \exp(-t/\tau_1) \ , \tag{11}$$

where τ_1 is the mean time between the trapping events, or $1/\tau_1$ is the trapping rate. The time derivatives $-p'(t)\,dt$ and $-q'(t)\,dt$ give the probabilities that the hydrogen remains in the trapped state until the time t, and changes from the trapped state into the diffusing state within the time interval dt, and vice versa. The hydrogen alternates randomly between these two kinds of motion. Obviously, the self-correlation function for the trapped state is

$$G_{s0}(\vec{r},t) = \delta(\vec{r}) \tag{12}$$

neglecting the vibrations. The self-correlation function for the diffusive state $G_{s1}(\vec{r},t)$ is given by the solution of Eq. (3) for the undisturbed lattice. Assume now that a hydrogen starts for $t=0$ in the trapped state; then it can reach a certain site $\vec{r}$ at a time t, after having changed its state $0, 1, 2, \ldots, i$ times. The probability for such a path will be called $F_i^T(\vec{r},t)$, and one obtains

$$G_s^T(\vec{r},t) = \sum_{L=0}^{\infty} F_i^T(\vec{r},t) \ . \tag{13}$$

The particle can also start in the "free" state, and corresponding functions $F_i^F(\vec{r},t)$ and $G_s^F(\vec{r},t)$ are defined. The total self-correlation function $G_s(\vec{r},t)$ is then the thermal average of these two components, namely,

$$G_s(\vec{r},t) = \frac{\tau_0}{\tau_0+\tau_1} G_s^T(\vec{r},t) + \frac{\tau_1}{\tau_0+\tau_1} G_s^F(\vec{r},t) \ . \tag{14}$$

The functions F_i^T and F_i^F can be obtained by a procedure applied for the calculation of the scattering law for oscillatory diffusion.[14] After Fourier transformation of the functions F_i, the summation in Eq. (13) can be carried out. Using the notation of Singwi and Sjölander[14] one obtains

$$S_{\text{inc}}(\vec{Q},\omega) = \frac{\tau_0}{\tau_0+\tau_1}\left(\frac{A+BC}{1-CD}\right) + \frac{\tau_1}{\tau_0+\tau_1}\left(\frac{B+AD}{1-CD}\right) \ , \tag{15}$$

with

$$A = \int dt\, d^3r\, G_{s0}(\vec{r},t) \exp[i(\vec{Q}\cdot\vec{r}-\omega t)]$$

$$= \frac{\tau_0}{1+i\omega\tau_0} \ , \tag{16}$$

$$B = \int dt\, d^3r\, G_{s1}(\vec{r},t) \exp[i(\vec{Q}\cdot\vec{r}-\omega t)]$$

$$= \frac{\tau_1}{1+[\Lambda(\vec{Q})+i\omega]\tau_1} \ , \tag{17}$$

$$C = A/\tau_0; \quad D = B/\tau_1 \ . \tag{18}$$

A simple algebraic transformation leads to a two-component spectrum, namely,

$$S_{\text{inc}}(\vec{Q},\omega) = R_1 \frac{\Lambda_1/\pi}{\Lambda_1^2+\omega^2} + (1-R_1)\frac{\Lambda_2/\pi}{\Lambda_2^2+\omega^2} \ , \tag{19}$$

with

$$\Lambda_{1,2} = \tfrac{1}{2}(\tau_0^{-1}+\tau_1^{-1}+\Lambda(\vec{Q}) \pm \{[\tau_0^{-1}+\tau_1^{-1}+\Lambda(\vec{Q})]^2 - 4\Lambda(\vec{Q})/\tau_0\}^{1/2}) \ , \tag{20}$$

$$R_1 = \tfrac{1}{2} + \tfrac{1}{2}\left(\Lambda(\vec{Q})\frac{\tau_1-\tau_0}{\tau_1+\tau_0} - \tau_0^{-1} - \tau_1^{-1}\right) \times \{[\tau_0^{-1}+\tau_1^{-1}\Lambda(\vec{Q})]^2 - 4\Lambda(\vec{Q})/\tau_0\}^{-1/2} \ . \tag{21}$$

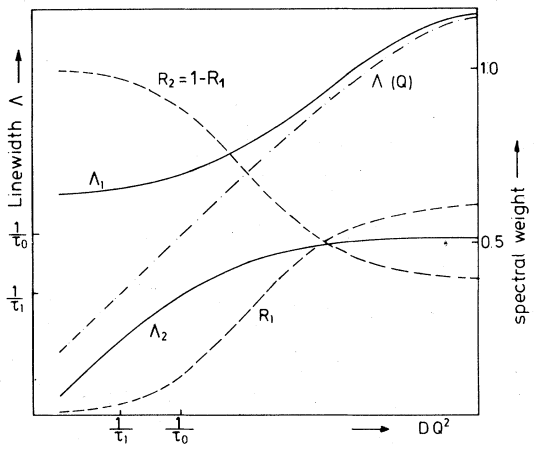

FIG. 2. Linewidth of the two components Λ_1 and Λ_2 (solid line, double logarithmic scale) and their spectral weights (dashed line) in the scattering law of the random-walk model, calculated for the first Brillouin zone of a simple cubic lattice. Dashed-dotted line: linewidth $\Lambda(Q)$ in the undisturbed lattice.

To illustrate the typical features of the scattering law, Fig. 2 represents the behavior of its two components, namely their widths $\Lambda_{1,2}$ and weights $R_{1,2}$, as a function of Q for a simple cubic lattice. The quantities have been calculated for a (1,1,1) direction and scaled by the jump rate $1/\tau$ of the undisturbed lattice, chosing $\tau_0/\tau = 6$ and $\tau_1/\tau = 12$ as an example.

For small Q the scattering intensity is determined by an average over a long section of the diffusive path, and according to Eq. (19) it is dominated by a Lorentzian-shaped quasielastic line. Its width is determined by the effective diffusion coefficient in the host lattice with impurities,

$$\Lambda_2 = D\frac{\tau_1}{\tau_0+\tau_1}Q^2 = D_{\text{eff}}Q^2 \quad , \tag{22}$$

with the effective diffusion coefficient

$$D_{\text{eff}} = D\frac{\tau_1}{\tau_0+\tau_1} \quad . \tag{23}$$

A small admixture of another Lorentzian appears, with a width $\Lambda_1 = \tau_0^{-1} + \tau_1^{-1}$ and a weight R_1 which is proportional to Q^4. On the other hand, for Q approaching the zone boundary, the spectrum is essentially related to the single diffusive steps. Equation (19) leads to two Lorentzians, a narrow one whose width is given by the escape rate $1/\tau_0$, and a broad one whose width is essentially determined by the jump rate in the undisturbed lattice. The weight of the *narrow* component is proportional to the thermal occupation of the traps. Deviations from the asymptotic Q^2 dependence according to Eq. (22) appear as soon as DQ^2 is comparable with $1/\tau_0$ or $1/\tau_1$. In this region, the Lorentzian with the width Λ_1 comes into play. We point out, that the jump-diffusion model used for the derivation of the scattering law applies for a Bravais lattice. Actually, H in Nb occupies six sublattices. For the region of small Q where our "black box" approximation is being used, the detailed sublattice structure does not come into play.

It should be noted that Eq. (23) is consistent with the simple reaction theory for diffusing particles[15] which leads to

$$D_{\text{eff}} = D/(1+4\pi c_t R_t D\tau_0) \quad , \tag{24}$$

where c_t is the trap concentration and R_t is the capture radius of the trap. Using the relation for the trapping rate of a totally absorbing trap[16]

$$1/\tau_1 = 4\pi R_t D c_t \quad , \tag{25}$$

Eq (24) leads immediately to our result Eq. (23). The quantity τ_1 can also be related to the mean-square distance between two trapping events, namely,

$$\langle s^2\rangle = 6D\tau_1 \quad . \tag{26}$$

The results of the two-state random-walk model, Eqs. (19)–(21) agree formally with the average T-matrix approximation.[17] Thus our procedure is justified by the theory of random defects. In addition, the ATA calculations relate the model parameters τ_0 and τ_1 to microscopic quantities of the diffusion process and the trap concentration.

In the *elastic interaction model* a *spectrum* of trapping times is introduced, in contrast to the RWM with one mean rest time only. This is achieved by the explicit introduction of an interaction potential between the impurity and a dissolved hydrogen. This potential is formulated in terms of two contributions: the short-range electronic force is approximated by a hard-core repulsion of radius r_0. For larger distances r, the interaction is attributed to an elastic strain field in a continuum approximation. Such a description has been successfully applied in many instances. (e.g., Refs. 18–20). This elastic interaction potential can be attractive or repulsive, depending on the position of the hydrogen atom relative to the impurity site, and it is zero in the orientational average. This potential can be written as[21]

$$V(\vec{r}) = -(1/r^3)[A^{\text{H}}A^{\text{N}}f_1(\vec{\Omega}) + A^{\text{H}}Q^{\text{N}}f_2(\vec{\Omega})] \quad , \tag{27}$$

for $r > r_0$. A^{H} and A^{N} are the diagonal components of the double force tensor which are related to the interaction strength of the dissolved hydrogen or nitrogen atom with the host lattice. The first term in Eq. (27) is related to the anisotropy of the host lattice. The second term is caused by the anisotropy of the double force tensor of the N atom which is described by the quantity Q^{N}. The orientation-dependent functions f_1 and f_2, together with the numerical values to be used in Eq. (27), are quoted in the Appendix. The hard-core radius will be used as the only disposable parameter of the model.

With this potential the change of the binding energy for the proton and of the activation energy for diffusive jumps will be calculated under the following assumption: the interaction between the nitrogen impurity and the hydrogen affects only the ground-state energy of the dissolved hydrogen, but *not* the saddle point of the potential between the interstitial sites. Therefore, the lowering of the groundstate is equal to the increase of the activation energy for diffusive jumps. This implies that the jump probability is the same for all directions and there is *no diffusive drift* around the impurity. Evidence of the validity of this assumption will be given at the end of Sec. IV.

Due to the elastic interaction between the H and N atoms, the ground-state energy of a large number of interstitial H sites around the impurity is affected. Therefore, for the spectrum of relaxation rates in the trapping region, a continuous distribution of H sites was supposed to be a good approximtion. A more de-

tailed formulation would make no sense since it is not clear whether, in the neighborhood of the impurity, the hydrogen still occupies tetrahedral sites.[8] For a distance $\bar{r}$ between nitrogen and hydrogen, the mean rest time is then given by

$$\tau(\bar{r}) = \hat{\tau} \exp[-\beta V(\bar{r})] \ , \tag{28}$$

where $\hat{\tau}$ is the mean rest time in the undisturbed lattice. Correspondingly, the thermal population is given by

$$\rho(\bar{r}) = \exp[-\beta V(\bar{r})] / \int d^3r \exp[-\beta V(\bar{r})] \ . \tag{29}$$

For diffusion without drift the self-diffusion constant in the impurity-doped lattice can be calculated[12] yielding

$$D_{\text{eff}} = l^2/6\bar{\tau} \ , \tag{30}$$

where l is the jump distance. The average rest time is given by

$$\bar{\tau} = \hat{\tau} \int d^3r \exp[-\beta V(\bar{r})] \Big/ \int d^3r \ . \tag{31}$$

In Sec. IV the Eqs. (30) and (31) will be applied to interpret the experiments at *small* scattering vectors Q. For larger Q, Eq. (3) had to be solved for the impurity-doped lattice, which is an extremely complicated task, and no simple approximation is possible. However, for Q near the zone boundary, the scattering law may be approximated by a superposition of Lorentzians whose widths and weights are given by the lifetime and thermal population of the different sites in the disturbed host lattice. This approximation was found to be very good in the case of the RMW [see Eqs. (20) and (21)]. For a distribution of trapping times, our assumption should hold as long as there is no drift of the hydrogen near the trap. With this approximation, the scattering law for Q near the zone boundary reflects the spectrum of relaxation rates $1/\tau(\bar{r})$. It is given by

$$S_{\text{inc}}(Q,\omega) = \int d^3r \, \rho(\bar{r}) \frac{\tau(\bar{r})^{-1}/\pi}{\tau(\bar{r})^{-2} + \omega^2} \Big/ \int d^3r \, \rho(\bar{r}) \ . \tag{32}$$

For such a scattering law, consisting of many Lorentzians with a wide spectrum of widths, the *observed* spectrum depends strongly on the resolution of the spectrometer. This aspect has been discussed in detail by Kehr *et al.*,[12] where in particular the influence of resolution on the apparent activation energy of the line-width has been studied. ("Apparent activation energy" of a quantity Γ means the slope of $\ln\Gamma$ vs $1/T$ in a given temperature range.)

III. EXPERIMENT

A. Sample

The quasielastic neutron scattering experiments were performed on two different samples I and II having different N and H concentrations. Each sample consisted of a bundle of 250 niobium wires (1.6-mm diam, 30-mm long). In addition, two identical NbN_x samples without hydrogen were prepared, in order to subtract the scattering from the host lattice, and the scattering on the N atoms with their strain fields.

The samples were prepared in four steps: (i) purification of the starting material: 1/2-in. 99.99% pure Nb rods, from which 1.5-mm wires were produced. Annealing of the lattice defects; (ii) nitrogen doping; (iii) quenching of the nitrogen-doped sample; and (iv) hydrogen loading. The wires were decarborated by dc heating in an oxygen atmosphere of 3×10^{-6} Torr during 1 h. Thereafter the wires were degassed at 2300 °C and a pressure below 10^{-10} Torr for 3 h, yielding residual resistivity ratios of about 2000. Inspection by electron microscope of similarly treated samples yielded dislocation densities below 10^5 cm^{-2}.[22]

Sieverts law relates the equilibrium concentration of the dissolved nitrogen at a given temperature to the partial nitrogen pressure. The Sieverts coefficients for the NbH system are known[23] yielding the order of magnitude for temperature and pressure to be chosen during N doping. In order to control the nitrogen concentration by residual resistivity measurements, additional experiments on nitrogen doping at different pressures were performed. The nitrogen content was determined by weighing. The resulting value for the specific residual resistivity was 4.0 $/\mu\Omega$ cm/(at.% N) in good agreement to earlier measurements.[24] The doping was carried out at 1.720 °C (sample I) and 1.800°C (sample II) during 2.5h in an atmosphere of 10^{-5}-Torr N. Altogether 35 m of Nb wire were doped. By switching off the current, quenching down to about 500 °C occurred within 20 sec. Essentially, our conditions of preparation were comparable with those applied by Gebhardt *et al.*[24] For sample I the N concentrations varied between 0.62 and 0.81 at.%, and for sample II between 0.27% and 0.46%. From this material the wires closest to the nominal N-concentration c_N were chosen for subsequent hydrogen loading.

Also the hydrogen loading was carried out from the gas phase and all wires were loaded simultaneously. (Electrolytic loading failed because it was impossible to control the hydrogen concentration during charging.) To be sure that there was no serious formation of nitrogen precipitates, the behavior of the nitrogen-doped wire after annealing at 500°C during times between 0.5 and 2 h, was studied by different investigations. (a) Electric measurements showed that the residual resistivity of the wires did not change during

the first hour of annealing. Thereafter, only a small decrease was found. This result agrees with observation of Gebhardt *et al.*[25] on NbN_x foils. (b) N-doped Nb foils were investigated by electron microscope before and after annealing at 500 °C during 1 h. No indication of NbH_x precipitations or formation of subnitrides (superstructure reflections) were seen. This is consistent with observations of Schober[26] which have shown that subnitride precipitates first appear for nitrogen concentrations higher than 1 at.%, and with results of Jung[27] on $TaN_{0.012}$ which yielded a drastic reduction of the residual resistivity after precipitation of TaN_x subnitrides. Summarizing these results and also including other investigations,[24–27] a larger amount of precipitation of subnitrides after annealing can be excluded. (c) The electric resistivity measurements might have missed small and coherent N clusters. Such clusters can be observed by a reduction of the Snoek relaxation strength. After annealing for 1 h, a decrease of the Snoek relaxation strength of about 20% was found. This means that the annealing may be responsible for the growth of clusters containing not more than 20% of the N atoms. Consequently, by hydrogen doping only during 20 min. at 500 °C, a much smaller effect is to be expected.

After hydrogen loading the hydrogen concentration was controlled by outgassing eight representative wires from each sample, yielding H concentrations of 0.391 at.% $\leq C_{\mathrm{H}} \leq$ 0.397 at.% (I) and 0.28 at.% $\leq C_{\mathrm{H}} \leq$ 0.34 at.% (II). The final composition of the samples used in the scattering experiment was: Sample I: $c_{\mathrm{H}} = 0.395 \pm 0.004$ at.%, $c_{\mathrm{N}} = 0.70 \pm 0.04$ at.%; sample II: $c_{\mathrm{H}} = 0.31 \pm 0.03$ at.%, and $c_{\mathrm{N}} = 0.37 \pm 0.03$ at.%. The reference samples had a nitrogen concentration of (I) $\bar{c}_{\mathrm{N}} = 0.7$ at.% and (II) $\bar{c}_{\mathrm{N}} = 0.37$ at.%, respectively. In order to reduce the incoherent background, both the heat shield of the cryostat and the sample holder were made of niobium.

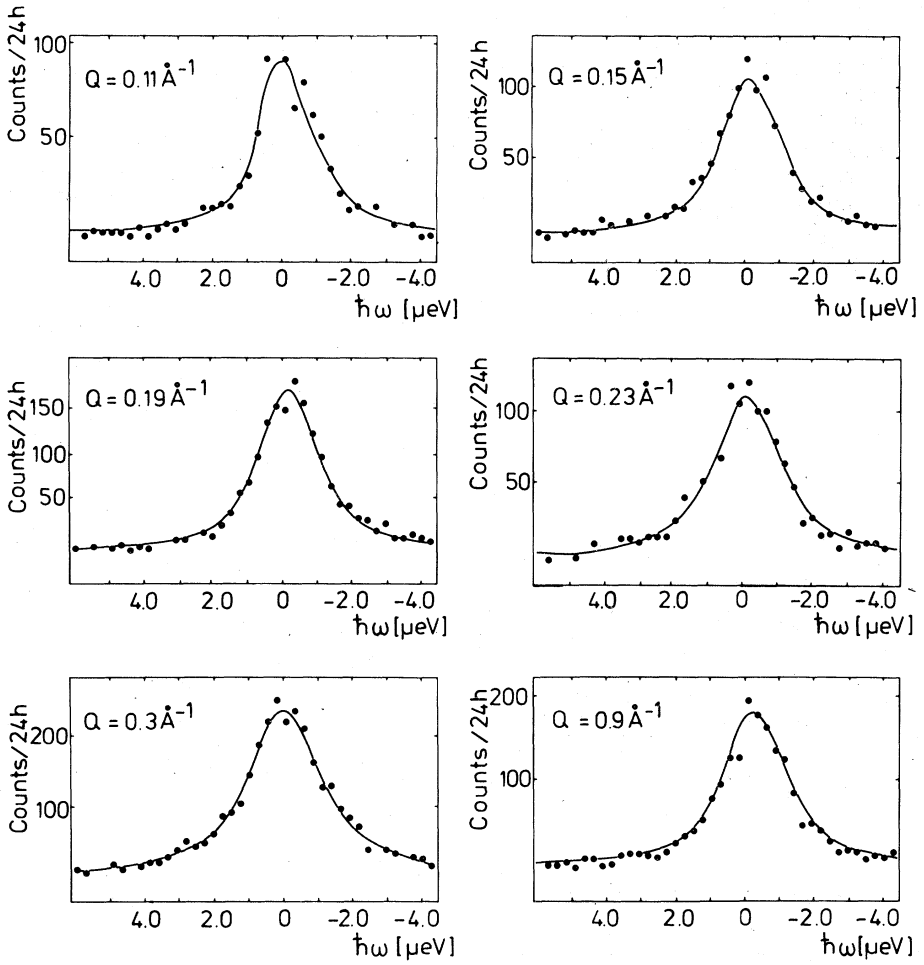

FIG. 3. Experimental spectra after background correction obtained for sample II at $T = 227$ K. Solid line: result of the fitting procedure with the random-walk model.

B. Measurements and results

The measurements were carried out with the backscattering spectrometer IN10,[28] at the Grenoble high-flux reactor. On sample I, spectra at six different and equidistant Q values were investigated between 0.15 and 1.9 Å^{-1} at each temperature. The measurements on sample II were mainly restricted to $0.1 \leq Q \leq 0.3$ Å^{-1} in order to check the small-Q behavior of the random-walk model. The energy range covered by the measurement ("energy window") was ± 5.3 μeV in both cases. The instrumental resolution was obtained from a measurement at 80 K. At this temperature the spectra are practically elastic, and the total scattering intensity I_0 falls entirely within the energy window of the spectrometer. This measurement was also used for the normalization of the intensities at high temperatures. The instrumental background was determined simultaneously with the scattering intensity from the reference samples.

The quasielastic spectra were measured at eight temperatures between 180 and 373 K (sample I), and at five temperatures between 198 and 303 K (sample II) (see Fig. 3). After background subtraction the spectra were fitted with Lorentzians convoluted with the experimental resolution curve. The intensity in units of I_0 and the line width were the fit parameters. Figure 4 presents the Q dependence of the quasielastic width for sample I at different temperatures, together with the corresponding curve for hydrogen at low concentration in pure niobium. In contrast to the validity of the Q^2 law in pure niobium up to $Q \simeq 1$ Å^{-1}, in the doped sample deviations occur already for the smallest Q values under consideration. In particular, this can be seen for sample II in Fig. 5. Comparing pure niobium and sample I, the width at large Q (1.9 Å^{-1}) differs by two orders of magnitude at 300 K.

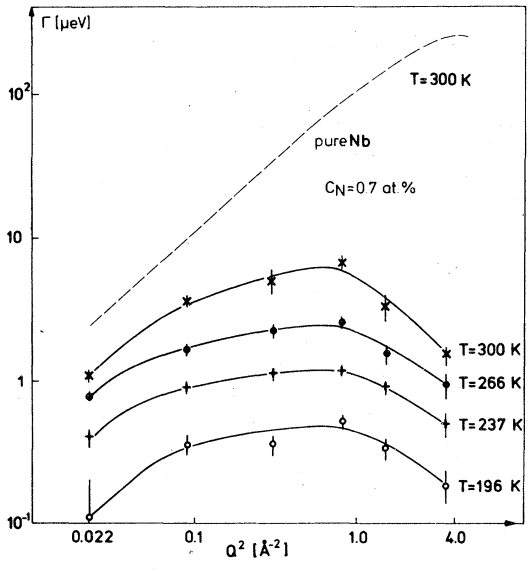

FIG. 4. Width Γ of the quasielastic neutron spectrum as a function of scattering vector Q and temperature T. Dashed line: H in pure niobium as extrapolated from data of Schaumann *et al.* (Ref. 29).

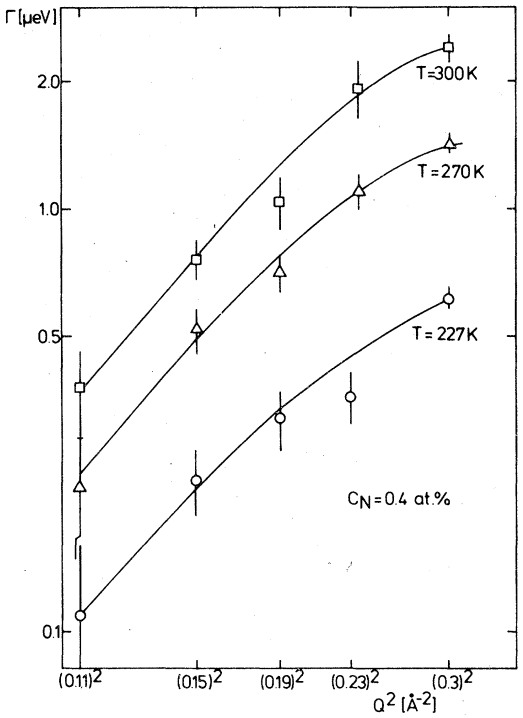

FIG. 5. Linewidth Γ of the quasielastic spectra measured on sample II as a function of the scattering vector Q and the temperature. Solid lines: guide lines for the eye.

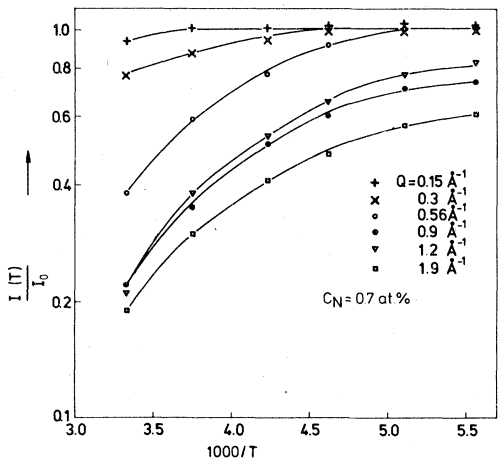

FIG. 6. Intensity of the observed quasielastic line, I at various Q values, in units of the total scattering intensity I_0.

Figure 6 shows the temperature dependence of the quasielastic intensity $I(T)$ as obtained from the integration of S_{inc} over the energy window ± 5.3 μeV, in units of the total intensity I_0. For small Q, nearly the full intensity is concentrated in the energy window. (The change of the total quasielastic intensity due to the Debye-Waller factor was estimated to be less than 1.5%.) However, at larger Q, only a fraction of the intensity appears in the integration window. The ratio I/I_0 decreases as the temperature increases. This behavior is due to the reduction of the fraction of trapped protons, and the intensity loss represents the increasing fraction of the freely diffusing protons.

Figure 7 shows an Arrhenius plot of the width at

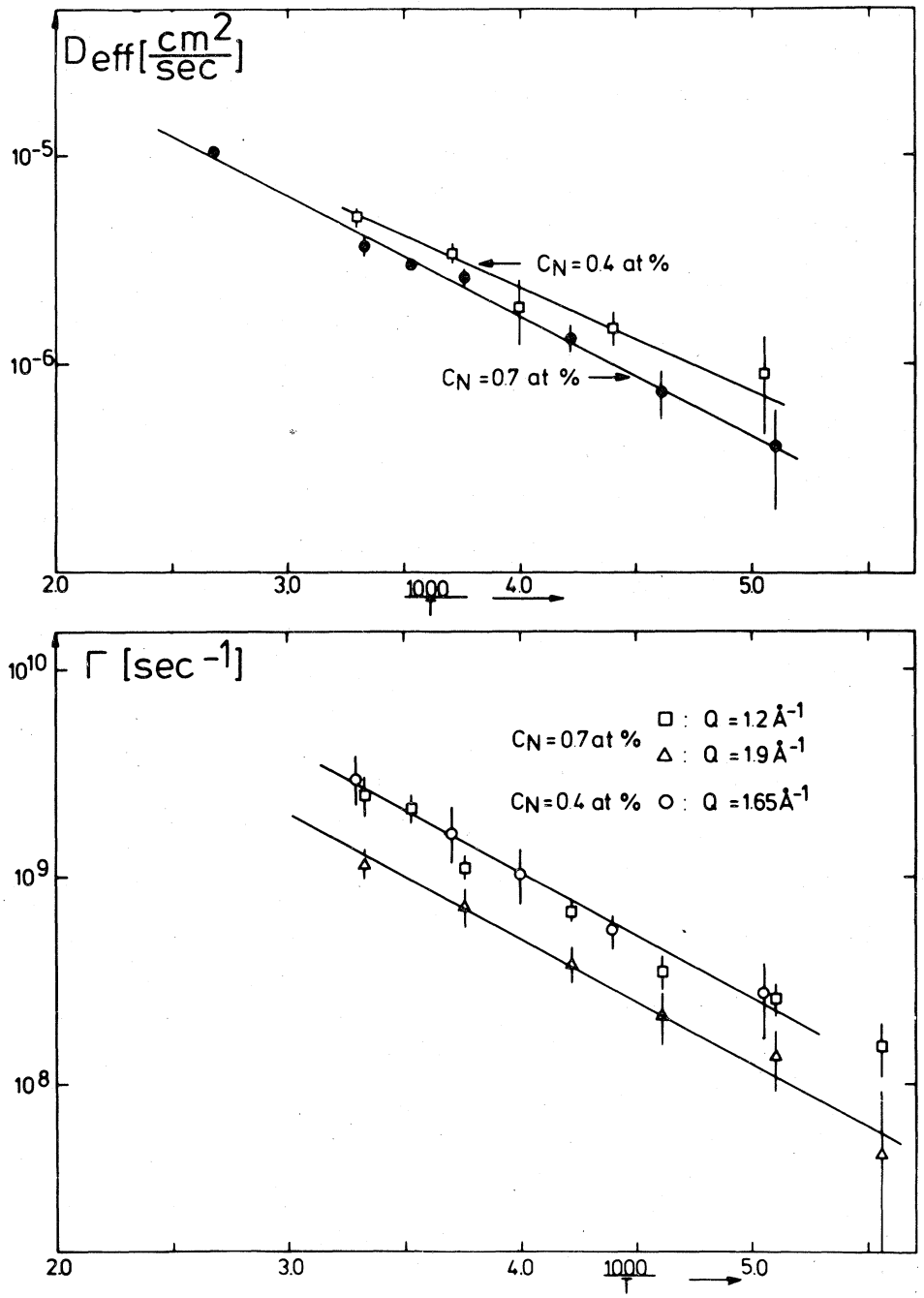

FIG. 7. Self-diffusion coefficient D_{eff} (from the quasielastic linewidth at the smallest measured Q value) and width of the spectrum at large Q for both nitrogen concentrations, as a function of temperature.

larger Q, and the quantity $D_{\text{eff}} = \Gamma/Q^2$ for small Q [Eqs. (9) and (23)]. The width at large Q can be described by a single activation energy in the whole temperature region. This holds as well for the diffusion coefficient D_{eff}, in contrast to pure niobium[29,30] where the apparent activation energy changes near 250 K. The activation energy of the width at $Q = 1.9$ Å^{-1} is 118 ±12 meV. At first sight this value is unexpectedly small in view of the sum of binding and activation energy in pure niobium (about 180 meV). This point will be discussed in Sec. IV.

IV. DISCUSSION

A. Random-walk model

For small Q, the observed Q dependence of the line width (see Figs. 4 and 5) agrees qualitatively with the behavior predicted by the RWM (Fig. 2): for Q between 0.15 and 0.2 Å^{-1}, the line width vs Q^2 already bends and approaches much smaller values than those obtained for H in the pure host lattice (dashed curve).

On the other hand, the experimental width in Fig. 4 passes through a maximum at about 1 Å^{-1}, whereas the calculated width increases monotonically. This discrepancy is presumably caused by the internal structure of the trap which is not taken into account in the RWM, and which comes into play as soon as $2\pi/Q$ is comparable with the dimension of the trap. Therefore, in our comparison with theory, only the experimental spectra for $Q \lesssim 0.9$ Å^{-1} were taken into account.

For sample I, four spectra were considered, and six spectra for sample II. At each temperature, the resolution-broadened spectra were calculated according to Eq. (19). They were simultaneously fitted for all Q values, using τ_0 and τ_1 as the only disposable parameters. The intensity was calibrated by the 80 K experiment. D vs T for pure niobium was taken from Gorski effect measurements[29] and from quasielastic scattering experiments.[30] The solid curves in Fig. 3 present the resolution broadened theoretical spectra according to this fitting procedure. Figure 8 shows the rates τ_0^{-1} and τ_1^{-1} in an Arrhenius representation which can be written as

$$\tau_0^{-1} = 2.6 \times 10^{12} \exp[-166(meV)/k_B T] \quad (sec^{-1}) \ , \tag{33}$$

for both N concentrations,

$$\tau_1^{-1} = 6.1 \times 10^{10} \exp[-93(meV)/k_B T] \quad (sec^{-1}) \ , \tag{34}$$

for $c_N = 0.7$at.%, and

$$\tau_1^{-1} = 3.6 \times 10^{10} \exp[-94(meV)/k_B T] \quad (sec^{-1}) \ , \tag{35}$$

for $c_N = 0.4$ at.%.

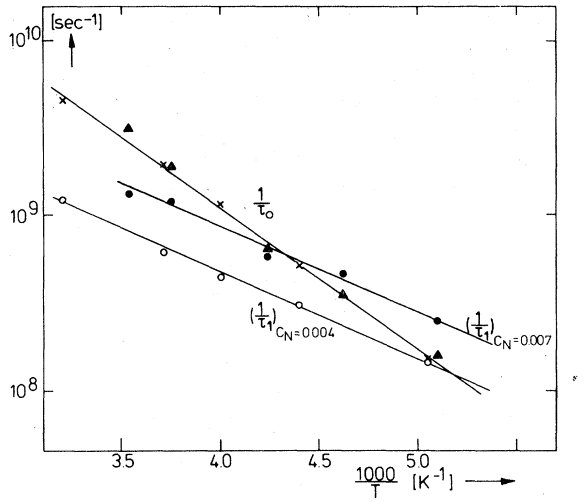

FIG. 8. Escape rate $1/\tau_0$ and trapping rate $1/\tau_1$ as a function of temperature for both nitrogen concentrations. For $1/\tau_0$, triangles correspond to $c_N = 0.007$, crosses to $c_N = 0.004$.

All fitting parameters are summarized in Table I. The results demonstrate that the random-walk model allows an accurate and consistent description of the experimental results. In particular the following features should be noted.

(i) The escape rate $1/\tau_0$ does not depend on the nitrogen concentration, as expected since τ_0 is a property of the single trap.

(ii) According to the random walk model, the activation energy for $1/\tau_0$ should be the sum of the binding energy and the activation energy for diffusion in pure niobium. Consequently, the ratio $\hat{\tau}/\tau_0$ should reveal an activation energy which is equal to the binding energy. Taking $\hat{\tau}$ from the experimental values of D vs T for pure niobium,[29,30] an activation energy for $\hat{\tau}/\tau_0$ of 90 meV is obtained. This agrees quite well with the results of internal friction experiments.[6]

(iii) From Eq. (25) the activation energy of τ_1 should agree with the activation energy of the self-diffusion constant D. However, the resulting values, according to Eqs. (34) and (35), are higher than the apparent activation energy for D in the temperature region under consideration (approximately 76 meV). The discrepancy can be explained by the assumption that the nitrogen impurities are saturated as soon as they have trapped a single hydrogen (see also Refs. 5 and 31). Under these circumstances, the effective trap concentration c_N^{eff} is smaller than c_N, and decreases with decreasing temperature. The intensity of the narrow quasielastic line for large Q, namely, $I(T)$, yields the fraction of the trapped hydrogen atoms. Consequently,

TABLE I. Results from fitting the data with the random-walk model for both nitrogen concentrations.

T (K)	C_N (at.%) 0.4	C_N (at.%) 0.7	$\frac{1}{\tau_0}$ (sec^{-1})	$\frac{1}{\tau_1}$ (sec^{-1})	$\frac{1}{\tau}$ (sec^{-1})[a]	$\frac{\tau_0}{\tau}$	$D_{\text{eff}}/D=\frac{\tau_1}{\tau_0+\tau_1}$
196		×	1.6×10^{8}	2.5×10^{8}	7.1×10^{10}	440	0.39
198	×		1.5×10^{8}	1.4×10^{8}	7.4×10^{10}	490	0.52
217		×	3.5×10^{8}	4.6×10^{8}	1.1×10^{11}	310	0.43
227	×		5.2×10^{8}	3.0×10^{8}	1.2×10^{11}	230	0.63
236		×	6.4×10^{8}	5.8×10^{8}	1.4×10^{11}	220	0.52
250	×		1.1×10^{9}	4.4×10^{8}	1.7×10^{11}	160	0.71
266		×	1.9×10^{9}	1.2×10^{9}	2.2×10^{11}	120	0.61
269	×		1.9×10^{9}	6.1×10^{8}	2.3×10^{11}	120	0.76
283		×	3.1×10^{9}	1.3×10^{9}	2.9×10^{11}	94	0.70
303	×		4.4×10^{9}	1.2×10^{9}	23.8×10^{11}	86	0.79

[a]The values for $1/\tau$ are taken from measurements on pure NbH (Refs. 29 and 30).

$$c_N^{\text{eff}}=c_N-[I(T)/I_0]c_H \quad . \tag{36}$$

This yields a renormalized trapping rate $\bar{\tau}_1^{-1}=\tau_1^{-1}(c_N/c_N^{\text{eff}})$. The apparent activation energy for this quantity, 81 meV for sample I, and 79 meV for sample II, agrees very well with the corresponding value of the activation energy for D in pure niobium.

(iv) Also the ratio of the capture rates

$$(\bar{\tau}_1^{-1})_{C_N=0.7\%}/(\bar{\tau}_1^{-1})_{C_N=0.4\%}=1.8\pm0.2 \tag{37}$$

agrees very well with the ratio of the concentration 1.9 ± 0.2, as predicted by the model [Eq. (25)].

The phenomenological parameter τ_1 or $\bar{\tau}_1$ can be easily correlated with the atomistic properties of the sample. $\bar{\tau}_1$ leads to the effective trapping radius R_T (see Table II). For an anisotropic potential one gets $uV(R_T)=k_BT$, where u follows from detailed theory[32] ($u\lesssim1$). Using the continuum approximation for the hydrogen-nitrogen interaction (see Appendix) and typical values of R_T in the (1,0,0) direction one obtains $V(R_T)\simeq30$ meV, which should be compared with $k_BT=17$–24 meV pertinent to our experiments. Furthermore, Eq. (26) yields the renormalized mean distance between the trapping events $\bar{s}$ obtained from $\bar{\tau}_1$. As expected, $\bar{s}$ is practically independent of the temperature, and rather close to the mean distance between the dissolved nitrogen atoms, namely, 14 Å (sample I) and 17 Å (sample II). On the other hand, s obtained from τ_1 increases if the temperature decreases (see Table II).

Using the values for τ_0 and τ_1 of Table I and D vs T from pure niobium,[29,30] Eq. (23) yields the effective self-diffusion coefficient, namely,

$$D_{\text{eff}}=3.9\times10^{-4}\exp[-110(\text{meV})/k_BT]\ \ (\text{cm}^2/\text{sec}) , \tag{38}$$

for $c_N=0.7$ at.% and

$$D_{\text{eff}}=3.1\times10^{-4}\exp[-101(\text{meV})/k_BT](\text{cm}^2/\text{sec}) , \tag{39}$$

for $c_N=0.4$ at.%. These values are consistent with the quasielastic width at small Q.

B. Elastic interaction model

Figures 9 and 10 compare the experimental points with the results of the elastic interaction model. The elastic parameters were taken as quoted in the Appen-

TABLE II. Trapping radius R_T, mean-free diffusive path s, and renormalized mean free path $\bar{s}$, for both nitrogen concentrations.

$C_N=0.4$ at.%				$C_N=0.7$ at.%			
T (K)	R_T (Å)	s (Å)	$\bar{s}$ (Å)	T (K)	R_T (Å)	s (Å)	$\bar{s}$ (Å)
198	5.6	26.4	20.3	196	4.8	19.3	15.9
227	5.9	23.4	19.8	217	5.2	18.0	15.3
250	5.8	22.8	19.9	236	4.8	18.2	15.8
269	5.2	22.6	21.0	266	6.1	15.4	16.2
303	5.9	20.6	19.9	283	4.8	17.2	15.9

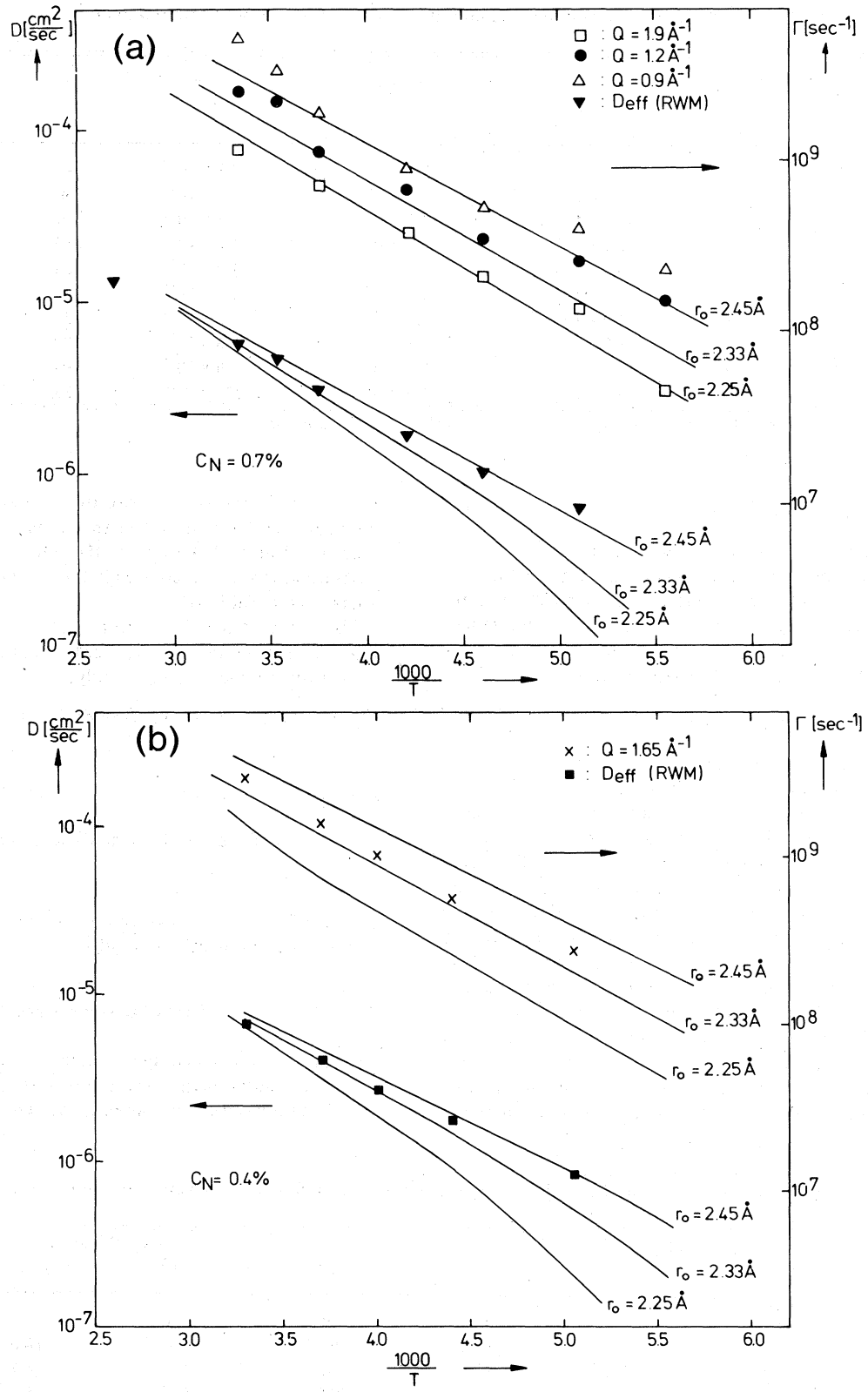

FIG. 9. Results of the elastic interaction model for different hard-core radii r_0, concerning the effective diffusion coefficient, D_{eff}, and the line width at large Q values, compared to the experimental values: (a) sample I; (b) sample II.

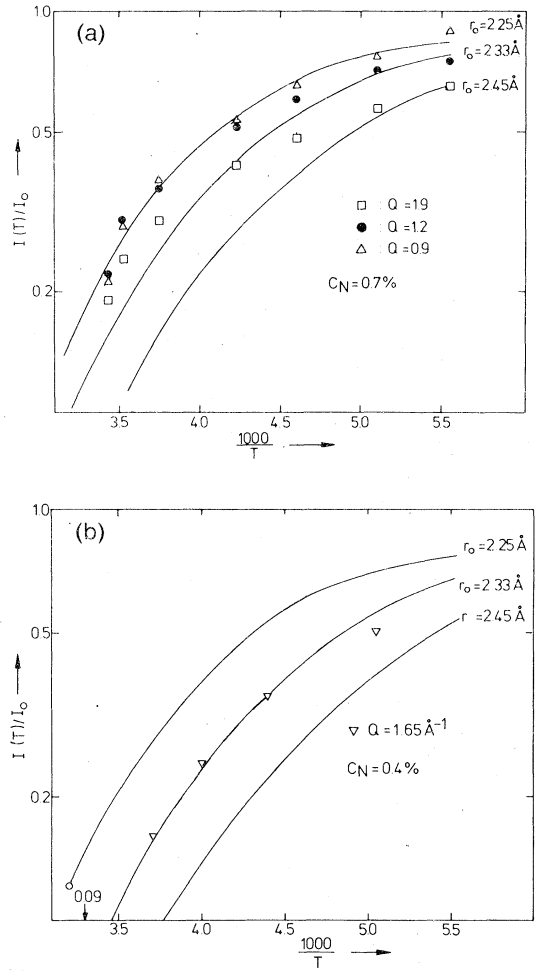

FIG. 10. Intensity of the observed quasielastic line for large Q values in comparison to the results of the elastic interaction model for different hard core radii: (a) sample I; (b) sample II.

dix. Obviously, good agreement is obtained for the width of the observed quasielastic line Γ at large Q, for the self-diffusion coefficient, D_{eff}, and for the relative intensity I/I_0 as a function of temperature. The only disposable parameter of the model, namely the hard-core radius r_0, was found to be in the order of 2.3 Å. It is noteworthy that this value coincides with the distance between the occupied tetrahedral sites in β-NbH_y.

In addition to the general agreement between theory and experiment, the following aspects deserve special attention. For pure NbH_y, the *slope* of $\ln D$ vs $1/T$ decreases if the temperature passes below 250 K.[29,30] For the doped sample, this change of the apparent activation energy disappears. This behavior was also observed by other authors.[4,30] From our calculations, this can be easily interpreted by the fact, that the decrease of the diffusion barrier in the undisturbed lattice is more or less compensated by the increasing efficiency of the traps. Accidentally, in our case the concave curvature of $\ln D$ vs $1/T$ is completely suppressed, and the curve behaves as if there were only a single activation energy. In general, for larger impurity concentration, or for impurities with higher binding energies, we expect a *convex* curvature of $\ln D$ vs $1/T$. Indications for such a behavior were found by Cantelli *et al.*[38] on highly impure Nb samples.

The observed small apparent activation energy for the measured width Γ at large Q is properly described by the elastic interaction model. Following Kehr *et al.*,[12] a small apparent activation energy results from a potential near the impurity, where the ground-state energies are affected, whereas the influence on the saddle point is small. As has been pointed out already, this implies that the drift motion does not play an important role. The experimental results justify this assumption which was made for our elastic interaction model. Recent computer simulations of the H diffusion in N-doped Nb[33] strongly support this point of view, where the influence of different potential structures with and without drift motion on the temperature dependence of the apparent line width has been studied. Only in the case, where the drift motion does not play an important role, a small activation energy at large Q appears. A model with *isotropic* elastic interaction[10] is not able to interpret the experimental data at large Q. In addition, this model needs a second disposable parameter.

V. RESUMÉ

Incoherent quasielastic neutron scattering on hydrogen in niobium doped with nitrogen impurities yields information on the behavior of hydrogen diffusion in the presence of trapping centers. The following results have been obtained.

(i) For small scattering vectors Q, the quasielastic width gives the effective self-diffusion coefficient D_{eff} for hydrogen in the doped Nb sample. D_{eff} is considerably smaller than the self-diffusion coefficient D in pure Nb. The measured value agrees with Gorski effect measurements.

(ii) At large Q, the spectrum reveals a quasielastic line whose width is about two orders of magnitude smaller than the width for diffusion in pure Nb. The line intensity decreases with increasing temperature. This narrow line can be attributed to H atoms in a trapped state near the N impurities.

(iii) The width, shape and intensity of the spectrum as a function of scattering vector Q ($Q < 1$ Å^{-1}), temperature, and nitrogen concentration c_N was interpreted in terms of a random-walk model. It characterizes the diffusion by two model parameters, namely, $1/\tau_0$,

the mean escape rate of the hydrogen out of the trap, and $1/\tau_1$, the mean trapping rate. The activation energy of $1/\tau_0$, about 166 meV, agrees with the results of other measurements.[6,5] According to the theory, the activation energy for $1/\tau_1$ should agree with the activation energy for the hydrogen self-diffusion constant D in pure Nb. This agreement was obtained after applying a small correction with regard to the saturation of the traps. Also, the dependence of $1/\tau_1$ on c_N agrees very well with the predictions of the theory.

(iv) An atomistic model for the diffusive process was applied describing the H-N interaction in terms of the elastic strain field produced by the dissolved N, in addition to a hard-core repulsion acting at small distances. This model also gives a very good and consistent description of the spectra over the whole temperature region, for small Q and for Q near the zone boundary, at both c_N. In these calculations, the known elastic parameters of the Nb lattice, and the double force tensor of the dissolved N and H atoms were used. Two *ad hoc* assumptions were made to achieve this consistency, namely, a hard-core radius of $r_0 \simeq 2,3$ Å (which corresponds to the H-H distance in β-NbH), and the assumption that no drift of the diffusing H atoms occurs in the vicinity of the N atom.

(v) For $Q \simeq 1$ Å^{-1} the measured quasielastic width vs Q^2 shows a maximum which is not reproduced by the random-walk model. It is assumed that this is caused by the detailed atomistic structure of the trapping region which is not taken into account in the theory.

(iv) The apparent activation energy for the hydrogen-diffusion coefficient in pure Nb undergoes a change near 250 K which disappears if impurity atoms are added. This behavior can be understood in terms of the elastic interaction model, as a more or less accidental compensation of the decreasing slope of $\ln D$ vs $1/T$ by an increasing efficiency of the traps.

ACKNOWLEDGMENT

The authors are grateful to T. Schober, H. Wenzl, J. M. Welter, J. Völkl, K. H. Klatt, and R. Schätzler for the help during the laborious preparation and characterization of the samples, to A. Heidemann and J. Töpler for their help during the experiments. We wish to thank K. W. Kehr and R. H. Swendsen for many discussions and suggestions. Finally, we thank the Institut Laue-Langevin for the support which it has given to this work.

APPENDIX

Equation (27) describes the elastic interaction potential between the hydrogen and the nitrogen atom in niobium in first order of lattice anisotropy $d = c_{11} - c_{12} - 2c_{44}$, where c_{ij} are the elastic moduli of niobium. The functions $f_1(\vec{\Omega})$ and $f_2(\vec{\Omega})$ depend on the orientation of the N-H distance vector. They are given by

$$f_1(\vec{\Omega}) = (15d/8\pi\bar{c}_{11}^2)e^{(0)} , \tag{A1}$$

$$f_2(\vec{\Omega}) = (15/8\pi\bar{c}_{11})\tilde{e}^{(1)} . \tag{A2}$$

$\bar{c}_{ij}$ are the average elastic moduli, namely,

$$\bar{c}_{12} = c_{12} + \tfrac{1}{5}d; \quad \bar{c}_{44} = c_{44} + \tfrac{1}{5}d; \quad \bar{c}_{11} = \bar{c}_{12} + 2\bar{c}_{44} . \tag{A3}$$

$e^{(0)}(\vec{\Omega})$ and $\tilde{e}^{(1)}(\vec{\Omega})$ determine the angular dependence of the potential. For a nitrogen atom situated on an octahedral site $(0,0,\frac{1}{2})$[34] they are given by[35]

$$e^{(0)} = 0.6 - \sum_j \cos^4\alpha_j , \tag{A4}$$

$$\tilde{e}^{(1)} = \tfrac{2}{15}(1 - 3\cos^2\alpha^{(z)}) + (d/\bar{c}_{44})e^{(1)} . \tag{A5}$$

α_j are the angles with respect to the cubic axes of the distance vector $\vec{r}$ between the nitrogen and the hydrogen. $e^{(1)}$ is a complicated function of the α_j and is given explicitly in Ref. 21. Using $A^H = 3.8$ eV (the double force tensor of H in Nb is isotropic within the experimental error[29]), $A^N = 4.3$ eV, $Q^N = 8.9$ eV,[36] and the elastic moduli of Nb,[37] the potential was found to be

$$V(\vec{r}) = -1.7e^{(0)}/r^3 - 14.1\tilde{e}^{(1)}/r^3 (\text{eV}) \tag{A6}$$

(r in Å). It should be noticed that Eq. (A6) yields attractive and repulsive regions.

[1]J. Völkl and G. Alefeld, in *Diffusion in Solids, Recent Development*, edited by A. S. Nowick and J. J. Burton (Academic, New York, 1975).
[2]P. Kofstadt, W. E. Wallace, and L. J. Hyvönen, J. Am. Chem. Soc. 81, 5015 (1959).
[3]P. Kofstadt and W. E. Wallace, J. Am. Chem. Soc. 81, 5019 (1959).
[4]W. Münzing, J. Völkl, H. Wipf, and G. Alefeld, Scripta Metall. 8, 1327 (1975).
[5]G. Pfeiffer and H. Wipf, J. Phys. F 6, 167 (1976).
[6]C. Baker and H. K. Birnbaum, Acta Metall. 21, 865 (1973).
[7]P. Schiller and A. Schneiders, Phys. Status Solidi 29, 375 (1975).
[8]P. Schiller and H. Nijman, Phys. Status Solidi 31, K77 (1975).
[9]For an extended treatment, e.g., A. Seeger, D. Schuhmach-

er, W. Schilling, and J. Diehl, in *Vacancies and Interstitials* (North–Holland, Amsterdam, 1970).
[10]For preliminary results, see, D. Richter, J. Töpler, and T. Springer, J. Phys. F 6, L 93 (1976).
[11]L. van Hove, Phys. Rev. 95, 249 (1954).
[12]K. W. Kehr, D. Richter, and R. H. Swendsen, J. Phys. F 8, 433 (1978).
[13]C. T. Chudley, R. J. Elliott, Proc. Phys. Soc. 77, 353 (1960); for a review, see T. Springer, Springer Tracts Mod. Phys. 64, 50 (1972).
[14]K. S. Singwi and A. Sjölander, Phys. Rev. 119, 863 (1960).
[15]W. Schilling and K. Schroeder, *Consultant Symposium: The Physics of Irradiation Produced Voids,* Harwell, 9–11 September 1974, AERE-R7934, (Metallurgy Division AERE, Harwell, 1975), p. 212.
[16]T. R. Waite, Phys. Rev. 107, 463;107, 471 (1957).
[17]K. W. Kehr and D. Richter, Solid State Commun. 20, 477 (1976).
[18]R. Siems, Jül-Bericht, Jül-545-FN (1968) (unpublished).
[19]P. H. Dederichs and J. Pollmann, Jül-Bericht, Jül-836-FF (1972) (unpublished).
[20]G. Alefeld, in *Critical Phenomena in Alloys, Magnets and Superconductors,* edited by R. E. Mills *et al.* (McGraw-Hill, New York, 1971).
[21]J. Pollmann, Jül-Bericht, Jül-1023-FF (1973) (unpublished).
[22]H. Wenzl (private communication, 1976).
[23]E. Fromm and H. Jehn, Metallw. Techn. 19, 747 (1965).
[24]E. Gebhardt, W. Dürrschnabel, and G. Hörz, J. Nucl. Mater. 18, 119 (1966).
[25]E. Gebhardt, W. Dürrschnabel, and G. Hörz, J. Nucl. Mater. 18, 134 (1966).
[26]T. Schober (private communication, 1975).
[27]P. Jung and T. Schober, Scripta Metall. 9, 949 (1975).
[28]A. Heidemann, Int. Report, ILL Grenoble (1974) (unpublished).
[29]G. Schaumann, J. Völkl and G. Alefeld, Phys. Status Solidi 42, 401 (1970).
[30]D. Richter, B. Alefeld, A. Heidemann, and N. Wakabayashi, J. Phys. F 7, 569 (1977).
[31]T. Matsumotu, Y. Sasaki, and M. Hihara, J. Phys. Chem. Solids 36, 215 (1975).
[32]K. Schroeder, Jül-Bericht, Jül-1083-FF (1974) (unpublished).
[33]R. H. Swendsen, D. Richter, and K. W. Kehr (unpublished).
[34]D. Carstanjen, Lecture DPG meeting, March 19–23, Münster, 1975 (unpublished).
[35]J. D. Eshelby, Solid State Phys. 3, 79 (1956).
[36]R. Gibbala and C. A. Wert, in *Diffusion in Body Centered Cubic Metals* (American Society for Metals, Cleveland, Ohio, 1965).
[37]From, *American Institute of Physics Handbook,* edited by B. H. Billings and D. F. Beil (McGraw-Hill, New York, 1972).
[38]R. Cantelli, F. M. Mazzolai, and M. Nuovo, Phys. Status Solidi 34, 597 (1969).